

The Superconductivity, Intragrain Penetration Depth and Meissner Effect of $\text{RuSr}_2(\text{Gd,Ce})_2\text{Cu}_2\text{O}_{10+\delta}$

Y. Y. Xue, B. Lorenz, A. Baikalov, D. H. Cao, Z. G. Li, and C. W. Chu*
*Physics Department, and Texas Center for Superconductivity,
 University of Houston, Houston TX 77204-5002*

(Dated: February 1, 2008)

The hole concentration p (δ), the transition temperature T_c , the intragrain penetration depth λ , and the Meissner effect were measured for annealed $\text{RuSr}_2(\text{Gd,Ce})_2\text{Cu}_2\text{O}_{10+\delta}$ samples. The intragrain superconducting transition temperature T_c varied from 17 to 40 K while the p changed by only 0.03 holes/ CuO_2 . The intragrain superfluid-density $1/\lambda^2$ and the diamagnetic drop of the field-cooled magnetization across T_c (the Meissner effect), however, increased more than 10 times. All of these findings are in disagreement with both the T_c vs. p and the T_c vs. $1/\lambda^2$ correlations proposed for homogeneous cuprates, but are in line with a possible phase-separation and the granularity associated with it.

PACS numbers: 74.62.-c, 74.80.-q, 74.25.Bt

One key question about $\text{RuSr}_2\text{GdCu}_2\text{O}_{8+\delta}$ (Ru1212) and $\text{RuSr}_2(\text{Gd,Ce})_2\text{Cu}_2\text{O}_{10+\delta}$ (Ru1222), where the partially ferromagnetically (FM) aligned Ru-spins and the superconducting (SC) CuO_2 layers are structurally adjacent, is what determines their superconductivity. Different groups have emphasized either their underdoped nature (*i.e.* the hole-concentration $p \ll 0.16$ holes/ CuO_2) or the competition between the SC and the coexisting FM through the Fulde-Ferrell-Larkin-Ovchinnikov (FFLO) phase.^{1,2,3,4,5} A verification was difficult until the recent reports that the transition temperature T_c 's of Ru1222 and Ru1212 can be adjusted over a broad range by oxygen-annealing and Cu-substitution, respectively.^{6,7,8} The reported data, unfortunately, show that the T_c -enhancement is accompanied by both a p -increase and a suppression of the ferromagnetic spin-order, and offer no clear distinction. To explore the topic, we measured the intragrain T_c , the p , the intragrain superfluid-density $1/\lambda^2$, and the Meissner effect in several annealed Ru1222 samples. The data were then compared with both the T_c vs. p correlation,⁹ and the T_c vs. $1/\lambda^2$ line proposed.¹⁰ We observed that a two-fold enhancement of T_c (from 17 to 40 K) is accompanied by a relatively small change of p (from 0.09 to 0.12 holes/ CuO_2), but a 20-fold increase in $1/\lambda^2$ (from 0.3 to 6 μm^{-2}). Together with an extremely large field effect of $dT_c/dH > 100$ K/T and a linear increase of the Meissner fraction with $1/\lambda^2$, the data suggest that those ruthenocuprate grains are actually Josephson-junction-arrays (JJA), in agreement with the phase-separation model suggested.¹¹ Further investigations of local magnetic structures are needed to solve the problem.

Ceramic $\text{RuSr}_2(\text{Gd}_{0.7}\text{Ce}_{0.3})_2\text{Cu}_2\text{O}_{10+\delta}$ samples were synthesized following the standard solid-state-reaction procedure. Precursors were first prepared by calcined commercial oxides at 400-900 °C under flowing O_2 . Mixed powder with a proper cation ratio was then pressed into pellets and sintered at 900 °C in air for 24 hr. The final heat treatment of the ceramics was done at 1090 °C for 60 hr after repeatedly sintering and regrinding at 1000 °C. Powders with different particle sizes were prepared according to the procedures previously reported.¹² The structure of the samples was determined by powder X-ray diffraction (XRD), using a Rigaku DMAX-III B diffractometer. The XRD pattern of a typical sample is shown in Fig. 1. Refinement was done based on a space group of $I4/mmm$ with lattice parameters of $a = 3.839(1)$ and $c = 28.591(5)$ using the Rietan-2000 program.¹³ There are no noticeable impurity lines in the X-ray diffraction pattern within our resolution of a few percent. The grain sizes ($\approx 2\text{-}20$ μm) of the ceramic samples, as well as the particle sizes of the powders, were measured using a JEOL JSM 6400 scanning electron microscope (SEM). The magnetizations were measured using a Quantum Design SQUID magnetometer with an *ac* attachment.

The data from nine Ru1222 samples in three sets are presented here. A0, B0, and C0 are as-synthesized samples with slightly different superconducting transition temperatures between 26 and 30 K (probably due to the slight differences in the final heat treatment and the various resulting intragrain granularities). All others are pieces of the respective as-synthesized ceramic after a 2 hr/600 °C anneal. The gases used in annealing are 300 atm. O_2 for samples A1, B1, and C1; 20 atm. O_2 for sample A2; Ar+0.01 atm. O_2 for sample C2; and high purity Ar (99.99%) for sample C3. The zero-field-cooled magnetization (M_{ZFC}) and the field-cooled one (M_{FC}) of samples A0, A1, and A2 are shown in Fig. 2. A systematic increase of the T_c (defined as the major inflection point of the M_{ZFC} and marked by arrows in the figure) with the assumed oxygen-intake can be clearly seen, *i.e.* from 26 to 40 K.⁷ It should be pointed out that the T_c so-defined is actually the intragrain transition-temperature based on both the size- and the H_{ac} -dependencies of the *ac* χ measured in the same samples, where H_{ac} is the *ac* field used (Fig. 3).^{12,14} The intergrain transition of our Ru1222 samples is typically $\approx 10\text{-}20$ K lower, and a perfect shielding can be reached only under $H_{ac} \approx 0.01$ Oe (Fig. 3). This relatively weaker intergrain coupling of Ru1222 ceramic seems to be typical in

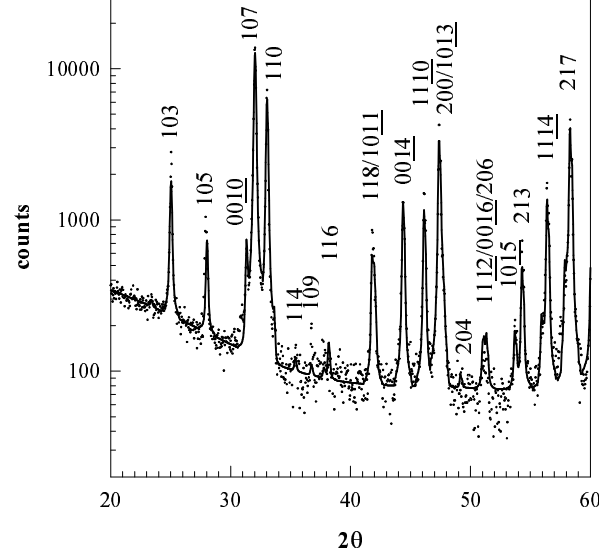


FIG. 1: The XRD of sample A0. dots: data; solid line: the refinement with $I4/mmm$.

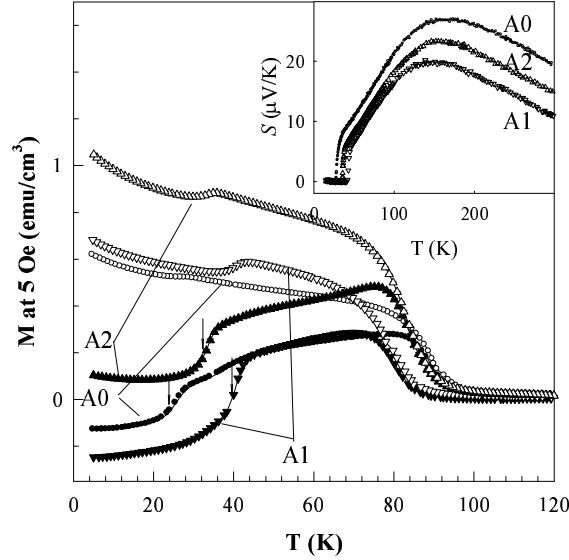


FIG. 2: The M_{ZFC} (solid symbols) and M_{FC} (open symbols) at 5 Oe for \bigcirc/\bullet : sample A0; $\nabla/\blacktriangledown$: sample A1; and \triangle/\blacktriangle : sample A2. Inset: Thermal power $S(T)$ of the three samples.

previously published reports, where a less than 100% shielding in M_{ZFC} was observed.^{7,15} We attribute this to the 1090 °C final heat-treatment temperature used, which is higher than that used for Ru1212.

To estimate the p , the thermoelectric power, S , was measured (inset, Fig. 2). The overall T-dependence of the S is similar to that of the underdoped $YBa_2Ca_3O_{7-\delta}$, and is in agreement with the data previously reported.¹⁵ No evidence of the RuO_2 contributions can be noticed.¹ A moderate increase of p (*i.e.* from 0.104 holes/ CuO_2 in sample A0 to 0.121 holes/ CuO_2 in sample A1) was then deduced using the proposed universal correlation of $S(290\text{ K}) = 992\exp(-38.1p)$.¹⁶ To verify the deduced p ,¹⁵ the oxygen-intake, $\Delta\delta$, was measured using a gas-effusion cell, where the sample was heated to 800 °C and the released oxygen was measured by both a pressure-gauge and a mass spectrometer.¹⁷ The total oxygen released is 0.1 and 0.115 O/Ru1222 for samples A0 and A1, respectively. While the absolute stoichiometry, $10+\delta$, may depend on the phase compositions at 800 °C, the $\Delta\delta$ should be less debatable. The

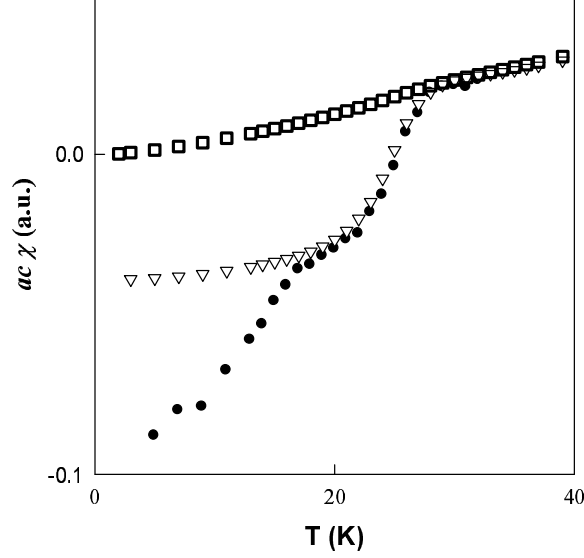


FIG. 3: $ac\chi$ of the bulk sample A0 (powders with particle size of 10 μm or larger show the same χ) under H_{ac} of 3 (∇) and 0.01 Oe (\bullet), as well as that at $H_{ac} = 3$ Oe of a 1 μm powder made from it (\square).

$\Delta\delta \approx 0.015$ so obtained is in good agreement with both the estimated p from S and the reported rate of $\Delta\delta/\Delta T_c \approx 0.0014$ O/K for Ru1222 with similar T_c .^{18,19} The expected T_c enhancement, however, should be less than 6 K based on the correlation of $T_c = T_{c,\text{max}}[1-82(p-0.16)^2]$ with $T_{c,\text{max}} \leq 50$ K.¹⁶ This value is far smaller than the 14 K enhancement observed, and the change in carrier concentration should not be the dominant factor.

It is interesting to note that the T_c -enhancement is accompanied by an increase in the diamagnetic drops (ΔM_{ZFC} , ΔM_{FC}) across T_c in both M_{ZFC} and M_{FC} . For example, the ΔM_{ZFC} is ≈ 0.15 , 0.2, and 0.3 emu/cm^3 at 5 Oe for samples A0, A2, and A1, respectively (Fig. 2).²⁰ Comparable trends can also be noticed in the data previously reported.⁷ We tentatively attribute the change in ΔM_{ZFC} to a decrease in $1/\lambda^2$ (actually $1/\lambda_{ab}^2$), and verify the interpretation by the direct measurement of the intragrain penetration-depths λ through the ac susceptibility of powders. Several powders were prepared from the same ceramic by sorted according to their particle sizes, and the λ was deduced from the size dependency of the χ observed. The details have been reported before.^{12,21} The previous data analysis procedure, however, was slightly modified here to simultaneously fit both the large magnetic background χ_m and λ . For a randomly-oriented power j ($=1\dots n$), which contains particles $i = 1\dots m$ with sizes of $d_{j,i}$, one has:

$$\chi_j = \sum_i \int \{ [1 - 6(\lambda_{ab}/d_{j,i}) \coth(d_{j,i}/2\lambda_{ab}) + 12(\lambda_{ab}/d_{j,i})^2] d_{j,i}^3 \cos^2\theta \sin\theta + [1 - 6(\lambda_c/d_{j,i}) \coth(d_{j,i}/2\lambda_c) + 12(\lambda_c/d_{j,i})^2] d_{j,i}^3 \sin^2\theta \sin\theta \} d\theta / \sum_i d_{j,i}^3 + \chi_m, \text{ where } \lambda_c, \lambda_{ab}, \text{ and } \theta \text{ are the penetration depths along } c, ab, \text{ and the polar angle, respectively. When } \lambda_c \gg \lambda_{ab} \text{ (highly anisotropy approximation) one has:}$$

$$\chi_j = \sum_i \{ [1 - 6(\lambda_{ab}/d_{j,i}) \coth(d_{j,i}/2\lambda_{ab}) + 12(\lambda_{ab}/d_{j,i})^2] d_{j,i}^3 / 3 \sum_i d_{j,i}^3 + \chi_m \}.$$

A regression was used to calculate λ without assumptions of χ_m . The χ_j of the powder with the smallest average particle size was used as the initial value of χ_m . The initial value of λ was deduced from the χ of the powder with the largest particle size. The new χ_m was then regressively calculated through a least-square fit using the approximate λ value and the χ_j , $d_{j,i}$ data observed. The regression of λ followed. Typically, the result will be convergent to within 1% after three regression cycles.

The procedure was tested on the data of $\text{YBa}_2\text{Cu}_3\text{O}_{6.6}$ and MgB_2 previously collected, and led to a good agreement with the values expected.^{12,21} The possible uncertainty of the λ seems to be less than 30%, mainly from the statistical uncertainty of d_i . As an example, the data of three powder-samples from ceramic A1 with effective particle-sizes of $d = 1.9$, 1.3, and 0.9 μm are shown in the inset of Fig. 4. Their χ , the deduced χ_m , and the fitting results are shown as symbols, a dashed line, and solid lines, respectively. The deduced superfluid densities, $1/\lambda^2$'s of samples A0 and A1 are shown in Fig. 4. The twofold increase of $1/\lambda^2$, which is in agreement with the raw M_{ZFC} data of both that in the Fig. 2 and that reported previously,^{7,8} confirms the above assumption that the change in $1/\lambda^2$ is the dominant factor for ΔM_{ZFC} and ΔM_{FC} . This view is further supported by an unusual large $dT_c/dH \approx 100$ K/T similar to that observed in Ru1212Eu (Fig. 5).

The increase in $1/\lambda^2$ is significantly higher than that expected from both the p and the T_c observed. In principle, the effective mass m^* , pair-breaking scatterings, and intragrain granularity can all affect the $1/\lambda^2$ observed. However,

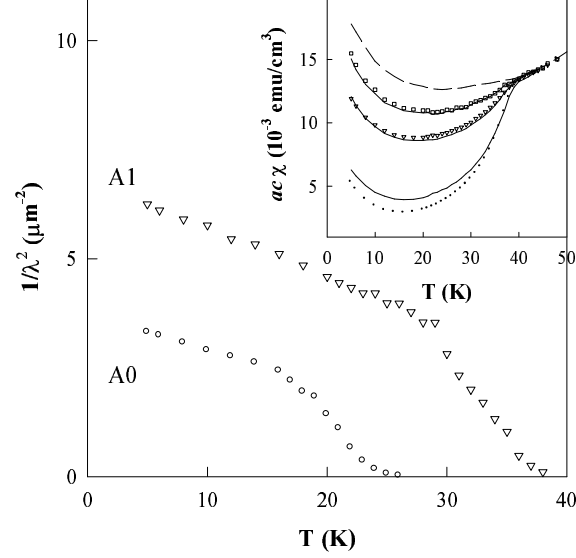


FIG. 4: The intragrain $1/\lambda^2$ for ∇ : sample A0 and \circ : sample A1. Inset: the $ac \chi$ of powder made from sample A1 with particle size of \circ : $1.9 \mu\text{m}$; ∇ : $1.3 \mu\text{m}$; and \square : $0.9 \mu\text{m}$. The solid lines are fits and the dashed line is the estimated magnetic background.

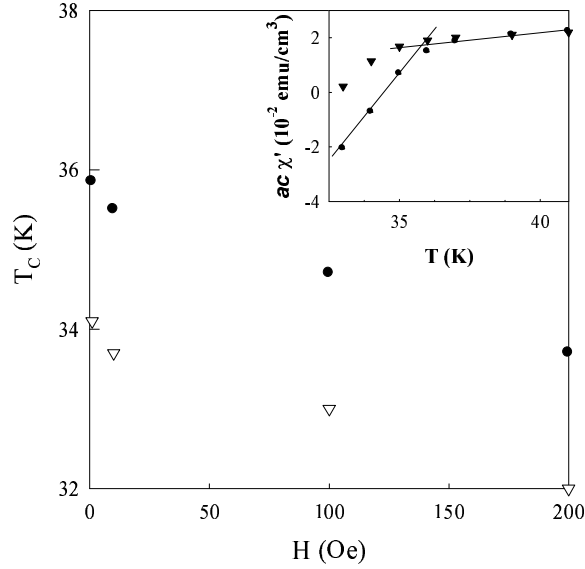


FIG. 5: The intragrain T_c , deduced as the onset of the differential χ (\bullet) and the inflection point of M_{FC} (∇). Inset. The differential susceptibility measured as the $ac \chi$ at $H_{ac} = 0.3 \text{ Oe}$ with a dc bias of 1 (\bullet) and 100 Oe (\blacktriangledown). The T_c is determined as the cross point of the linear fits (the solid lines) below and above T_c .

the comparable 300 K resistivity of the samples A0 and A1, *e.g.* ≈ 0.024 and $0.029 \Omega\text{cm}$ respectively, suggests that m^* may not play a major role here. To verify the possibility of the simple pair-broken mechanism, the $1/\lambda^2$'s of several samples with T_c ranging from 17 K (sample C3) to 40 K (sample A1) were measured (Fig. 6).²² In typical cuprates with pair-breakers (*e.g.* Zn), Nachumi *et. al.* have observed that T_c is a universal linear function of $1/\lambda^2$.¹⁰ Although there are still disputes about the data-details at high Zn-levels and their interpretation, all reported T_c data approach zero with the suppression of $1/\lambda^2$ with pair-breaking. In particular, both the strong-coupling *d*-wave model in the unitarity limit and the “swiss cheese” model predicts $T_c < 10 \text{ K}$ when $1/\lambda^2 \approx 0.3 \mu\text{m}^{-2}$ (*i.e.* $\sigma \approx$

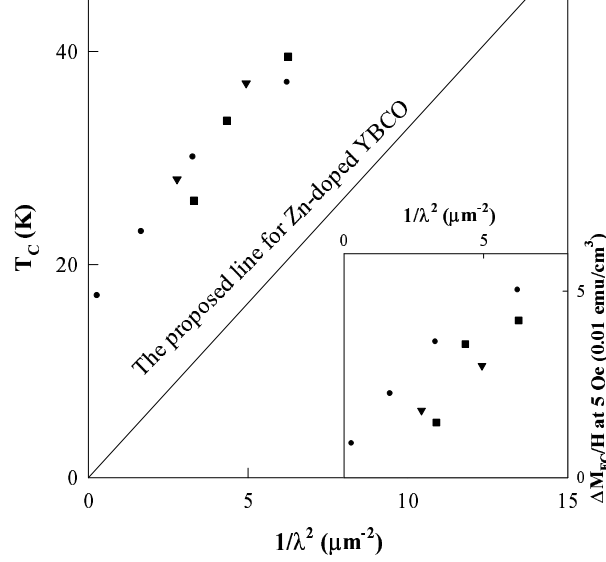


FIG. 6: T_c vs. $1/\lambda^2$ at 5 K for several annealed samples. Solid line: the Uemura line. Inset: the diamagnetic drop $\Delta M_{FC}/H$ across T_c at 5 Oe vs. $1/\lambda^2$. Symbols used are ■: A0-A2; ▼: B0-B1; ●: C0-C3.

$0.02 \mu s^{-1}$ in a μSR measurement).^{10,23} It is, therefore, interesting to note that all of our data points fall on the far left of this line. In particular, the T_c of sample C2 with $1/\lambda^2 \approx 0.3 \mu m^{-2}$ is still 15 K or higher. The trend is in line with the data of Ru1212, where samples with $\lambda(5 K)$ as large as $2-3 \mu m$ still have $T_c > 20 K$.¹² A simple pair-broken mechanism, therefore, may have difficulty in accommodating the data. This view is supported by the fact that there is no systematic correlation between the T_c (or $1/\lambda^2$) and the M_{FC} (or the remanent moment) above T_c , *i.e.* the FM aligned spins. In fact, the M_{FC} at 5 Oe and 50 K differs less than 5% between samples C3 and C1 with T_c of 17 and 37 K, respectively. The M_{FC} spread for samples A0, A1, and A2 is slightly larger, but again without a systematic dependency. A similar trend has also been pointed out previously in both the Ce-doped Ru1222 and the Cu-substituted Ru1212.^{8,15} Intragrain granularity, therefore, seems to be a more reasonable interpretation. It was proposed that the T_c of a JJA is $2.25J$, with J being the coupling energy of a junction.²⁴ The λ , in such a case, may depend on the length of the junctions involved, but the T_c will not. A non-zero phase-lock temperature, therefore, may coexist with an unusually long λ if the junction length is large.

Granularity of Ru1212 has been previously reported and attributed to either structural defects or possible phase-separation.^{1,2,12} However, no correlations between the T_c and the proposed 90° -rotated a - c microdomains (or the coherent rotation of the RuO_6 octahedrons) have ever been observed.^{1,25} We, therefore, favor a mesoscopic phase-separation between FM and AFM species as the origin of the granularity.^{11,26} The observation of a correlation between the magnetic transition temperature and the granularity (T_c , $1/\lambda^2$...) here certainly supports this view (Fig. 2). However, we will not discuss it further since it is not essential for the topics concerned, *i.e.* the evolution of T_c and Meissner effect with granularity.

The systematic increase of ΔM_{FC} , the Meissner effect, with annealing is also obvious in Fig. 2. The large Meissner fraction in a Ru1212 sample below 1 Oe and its disappear once above 10 Oe has previously been taken as evidence for a homogeneous superconductivity and a spontaneous vortex state (SVS), respectively.¹ The interpretation, in our opinion, is neither the only possible one nor the most likely one. Within the framework of the Ginzburg-Landau (G-L) model, the reversible part of ΔM_{FC} of a type II superconductor should have a maximum of $H_{c1}/4\pi$ at H_{c1} ; and a few times smaller ($\approx \frac{\phi_0 \ln(H_{c2}/H)}{32\pi^2 \lambda^2} = \frac{H_{c1} \ln(H_{c2}/H)}{8\pi \ln \kappa}$) in mixed states far above H_{c1} , where H_{c1} , H_{c2} , and κ are the lower- and upper-critical fields and the G-L parameter, respectively.^{27,28} This is simply the result of a competition between the magnetic energy $M \cdot H$ and the carrier kinetic-energy, and should hold even in the existence of spontaneous vortex and an internal magnetic field B_M ($= 4\pi M$ in homogeneous ferromagnetic superconductors). In particular, the ΔM_{FC} should be $\approx \phi_0 \ln \kappa / (16\pi^2 \lambda^2)$ ($> 1 \text{ emu/cm}^3$ with $\lambda < 0.5 \mu m$) over a broad H -range regardless of the value of B_M if the pinning is weak. The maximum ΔM_{FC} , we would argue, is a far better parameter for ferromagnetic superconductors than the widely used χ , whose interpretation may be ambiguous due to the uncertainties in the B_M and the possible SVS. The ΔM_{FC} of sample A1, for example, is $\approx 0.3 \text{ emu/cm}^3$ at 20 Oe, and seems to increase continuously with H although the large magnetic background makes a quantitative estimation difficult at larger fields.

This value is not too far from that expected based on the deduced $\lambda \approx 0.4 \mu\text{m}$, considering the corrections needed for the random grain-orientations and vortex pinning. The much smaller $\Delta M_{FC} < 0.04 \text{ emu/cm}^3$ over the whole H range reported) in Ref. 1, on the other hand, may imply a unusually long λ , *i.e.* severe granularity, if the pinning is not too strong.

It should be noted that a 100% Meissner effect can be reached in a JJA-like heterogeneous superconductor below its effective $H_{c1} \propto 1/\lambda^2$. The value of $\Delta M_{FC}/H$ is determined by both a free-energy balance and the vertex pinning. For the energy balance, all of the conclusions of Hao *et al.* should still hold if the JJA parameters are used.²⁷ In particular, a full Meissner effect can be expected below $\phi_o/(32\pi^2\lambda^2) \approx 1 \text{ Oe}$ with a λ as large as $2 \mu\text{m}$. The pinning strength, on the other hand, depends only on these parameters averaged over a length-scale of vortex cores. The $dT_c/dH > 100 \text{ K/T}$ observed in Ru1212 powders suggests that the cores of the related Josephson vertex may be as large as 10^{-2} - $10^{-1} \mu\text{m}$.¹⁴ The pinning, therefore, can be very weak if the sample can be regarded as homogeneous over such length-scales. The fact that full Meissner effects have been routinely observed in both underdoped and overdoped cuprates, where evidence for a possible mesoscopic phase-separation is accumulating,²⁹ supports the arguments. To verify this, the $\Delta M_{FC}/H$ of the nine samples at $H = 5 \text{ Oe}$ is plotted against their $1/\lambda^2$ at 5 K (inset, Fig. 5). The rough linear-correlation between the two parameters indicates that the Meissner effect $\Delta M_{FC}/H$ of Ru1222 is mainly determined by the intragrain Josephson penetration depth λ , at least for the samples examined here. Notice that the largest $\Delta M_{FC}/H$ observed here (0.06 emu/cm^3 at 5 Oe) is already a significant fraction of $1/4\pi$; a 100% Meissner effect below 1 Oe may not be sufficient evidence for microscopic-homogeneous superconductivity.

In summary, the intragrain T_c of Ru1222 has been tuned from 17 K to 40 K through O_2/Ar annealing. The corresponding change in the normal-state hole-concentration, however, is too small to account for the change. The associated intragrain $1/\lambda^2$, on the other hand, increases 20-fold, much more than that expected from the proposed T_c *vs.* $1/\lambda^2$ line for homogeneous cuprates. A Josephson-Junction-array model, therefore, is invoked to interpret the data. The increases in both T_c and Meissner effect with oxygen-intake in such a model are mainly due to the improvement of the intragrain granularity.

Acknowledgments

We thanks V. Diatschenko for careful read the manuscript. This work is supported in part by NSF Grant, the T. L. Temple Foundation, the John and Rebecca Moores Endowment and the State of Texas through TCSUH, and in LBNL by DOE.

-
- * Also at Lawrence Berkeley National Laboratory, 1 Cyclotron Road, Berkeley, CA 94720; and Hong Kong University of Science and Technology, Hong Kong
- ¹ C. Bernhard, J. L. Tallon, Ch. Niedermayer, Th. Blasius, A. Golnik, E. Brücher, R. K. Kremer, D. R. Noakes, C. E. Stronach and E. J. Ansaldo, Phys. Rev. B 59, 14099 (1999); C. Bernhard, J. L. Tallon, E. Brücher and R. K. Kremer, Phys. Rev. B61, 14960 (2000).
 - ² C. W. Chu, Y. Y. Xue, S. Tsui, J. Cmaidalka, A. K. Heilman, B. Lorenz and R. L. Meng, cond-mat/0002212 (2000).
 - ³ P. Fulde and R. A. Ferrell, Phys. Rev. 135, A550 (1964).
 - ⁴ W. E. Pickett, R. Weht and A. B. Shick, Phys. Rev. Lett. 83, 3713 (1999).
 - ⁵ J. X. Zhu, C. S. Ting and C. W. Chu, Phys. Rev. B 62, 11369 (2000).
 - ⁶ L. Baurnefeind, W. Widder and H. F. Braun, Physica C 254, 151 (1995).
 - ⁷ I. Felner, U. Asaf, Y. Levi and O. Millo, Physica C 334, 141 (2000); I. Felner, U. Asaf and E. Galstyan, cond-mat/0111217 (2001) and references therein.
 - ⁸ P. W. Klamut, B. Dabrowski, S. M. Mini, M. Maxwell, S. Kolesnik, M. Mais, A. Shengelaya, R. Khasanov, I. Savic, H. Keller, T. Graber, J. Gebhardt, P. J. Viccaro and Y. Xiao, Physica C364-365, 313 (2001); P. W. Klamut, B. Dabrowski, S. Kolesnik, M. Maxwell and J. Mais, Physica C364-365, 368 (2001).
 - ⁹ M. R. Presland, J. L. Tallon, R. G. Buckley, R. S. Liu and N. E. Flower, Physica C 176, 95 (1991).
 - ¹⁰ B. Nachumi, A. Keren, K. Kojima, M. Larkin, G. M. Luke, J. Merrin, O. Tchernyshov, Y. J. Uemura, N. Ichikawa, M. Goto and S. Uchida, Phys. Rev. Lett. 77, 5421 (1996); Phys. Rev. Lett. 80, 206 (1998) and references therein.
 - ¹¹ Y. Y. Xue, D. H. Cao, B. Lorenz and C. W. Chu, cond-mat/0109500 (2001).
 - ¹² Y. Y. Xue, B. Lorenz, R. L. Meng, A. Baikalov and C. W. Chu, Physica C364-365, 251 (2001).
 - ¹³ F. Izumi, Rigaku J., 6, 10 (1989).
 - ¹⁴ B. Lorenz, Y. Y. Xue, R. L. Meng and C. W. Chu, cond-mat/0107061 (2001).
 - ¹⁵ G. V. M. Williams and M. Ryan, Phys. Rev. B64, 094515 (2001).
 - ¹⁶ S. D. Obertalli, J. R. Cooper and J. L. Tallon, Phys. Rev. B46, 14928 (1992).

- ¹⁷ A. Hamed, R. Ortiz, H. H. Feng, Z. G. Li, P. H. Hor, Y. Y. Xue, Y. Y. Sun, Q. Xiong, Y. Cao, and C. W. Chu, Phys. Rev. B 54, 682 (1996).
- ¹⁸ K. D. Ottschi, T. Hinouchi, T. Mizukami, J. I. Shimoyama and K. Kishio, Advances in Superconductivity 12, 182 (2000).
- ¹⁹ Williams *et al.*¹⁵ reported a larger $\Delta\delta = 0.07$ O/Ru1222 with a comparable increase in T_c . The reason for the discrepancy is not known.
- ²⁰ The magnetic background apparantly chnages with annealing. In particular, the overall M_{ZFC} is positive for sample A2. However, its initial slope $dM_{ZFC}(5\text{ K})/dH$ (not shown here) is still negative. The thermopower reaches zero around T_c . In addition, both the dM_{ZFC}/dH and the ΔM_{ZFC} vary with the annealing systematically. We therefore attribute this to a change in magnetic background.
- ²¹ X. H. Chen, Y. Y. Xue, R. L. Meng and C. W. Chu, Phys. Rev. B64, 172501 (2001).
- ²² The p of these samples ranges from 0.09 to 0.12 holes/ CuO_2 based on the S measured.
- ²³ C. Bernhard, J. L. Tallon, C. Bucci, R. De Renzi, G. Guidi, G. V. M. Williams and Ch. Niedermayer, Phys. Rev. Lett. 77, 2304 (1996); Phys. Rev. Lett. 80, 205 (1998).
- ²⁴ Y. H. Li and S. Teitel, Phys. Rev. B40, 9122 (1989).
- ²⁵ A. C. McLaughlin, W. Zhou, J. P. Attfield, A. N. Fitch and J. L. Tallon, Phys. Rev. B60, 7512 (1999).
- ²⁶ V. G. Hadjiev, J. Bäckström, V. N. Popov, M. N. Iliev, R. L. Meng, Y. Y. Xue and C. W. Chu, Phys. Rev. B64, 134304 (2001).
- ²⁷ Z. D. Hao and J. R. Clem, Phys. Rev. Lett. 67, 2371 (1991).
- ²⁸ Some numerical coefficients at the order of unit are ignored here.
- ²⁹ See for example, H. A. Mook, P. C. Dai and F. Dogan, Phys. Rev. Lett. 88, 097004 (2002); H. H. Wen, X. H. Chen, W. L. Yang and Z. X. Zhao, Phys. Rev. Lett. 85, 2805 (2000).